Supporting Information

Burford et al. 10.1073/pnas.1300393110

SI Materials and Methods

β-Arrestin–Recruitment Assay. PathHunter human osteosarcoma cells (U2OS) expressing either μ-opioid receptors (U2OS-OPRM1) or δ-opioid receptors (U2OS-OPRD1), were grown in modified Eagle's medium containing 10% (vol/vol) FBS, 500 μg/mL G418, and 250 μg/mL hygromycin. Cells were grown to confluence in cell culture Nunc triple-layer flasks (Thermo Fisher Scientific), harvested with TrypLE Express, and resuspended in assay buffer (Hanks' buffered salt solution plus 25 mM Hepes, 100 IU/mL penicillin, 100 μg/mL streptomycin, 0.05% BSA at 1×10^6 cells/mL). Compounds (20 nL of 100× final concentration in 100% DMSO) were added to white, nontreated 1,536-well plates (Corning) by acoustic dispense using an Echo-550 (Labcyte) from Echo-qualified 1,536-well source plates (Corning). Next, 1 μL of assay buffer (agonist-detection mode), assay buffer containing a low concentration (~EC_{10}) of orthosteric agonist [positive allosteric modulator (PAM)-detection mode], or assay buffer containing an ~EC_{80} concentration of orthosteric agonist [antagonist/negative allosteric modulator (NAM)-detection mode] was added to assay plates. The orthosteric agonists used and their final concentrations are described in *Results*. Finally, 1 μL of cells (1,000 cells per well) in assay buffer was added to the wells to initiate the incubation period. Plates were lidded and incubated at room temperature for 90 min. Incubations were terminated by the addition of 1 μL of PathHunter reagent. One hour later, luminescence was detected using a Viewlux imaging plate reader (PerkinElmer). Additional characterization of certain μ-selective PAMs in the β-arrestin assay were performed essentially as described above using the various orthosteric agonist ligands and cell lines described in *Results*.

Inhibition of Forskolin-Stimulated cAMP-Accumulation Assays. CHO cells expressing recombinant human μ-opioid receptor (CHO-μ) were grown to confluence in F12 media containing 10% FBS, 100 IU/mL penicillin, 100 μg/mL streptomycin, and 400 μg/mL G418 in T-175 tissue culture flasks (Corning) and harvested with TrypLE Express. Cells were pelleted by centrifugation and resuspended in assay buffer at 6.67×10^5 cells per milliliter.

Compounds (30 nL of 100 × final concentration in 100% DMSO) were added to 1,536-well white, solid nontreated plates by acoustic dispense using an Echo-550. Next, 1.5 μL of assay buffer containing 1 mM 3-isobutyl-1-methylxanthine (IBMX) and 2× forskolin (final concentration, 1 μM), without (agonist-detection mode) or with (PAM-detection mode) 2× endomorphin-I (final concentration, 30 pM; an ~EC_{10} concentration) were added to the plates. Finally, cells (1.5 μL per well) were added to begin the incubation. Plates were incubated at room temperature for 30 min, followed by the addition of Cisbio homogeneous time resolved fluoresecence resonance energy transfer (HTRF) dynamic cAMP detection reagent (1.5 μL of D2-labeled cAMP tracer in lysis buffer, followed by 1.5 μL of Eucryptate–conjugated anti-cAMP antibody in lysis buffer). After a 1 h of incubation at room temperature, time-resolved fluorescence was detected on a Viewlux or Envision plate reader (PerkinElmer) with excitation at 337 nm and emission reads at 615 and 665 nm. The ratiometric data (665 nm read/615 nm read) × 10,000 was then converted to cAMP (nanomoles per liter) based on a standard curve for cAMP (replacing the cell addition step) run at the same time and under identical conditions to the assay.

Characterization of μ-selective PAMs in the CHO-μ cAMP assay, using curve-shift assays and probe-dependence assays, were performed as described above, using orthosteric agonists and modulators described in *Results*.

[^{35}S]GTPγS Binding Assay. Membranes were diluted with 50 mM Tris·HCl (pH 7.4) and preincubated with assay buffer containing GDP (1 volume membrane plus 2 volumes of 2× assay buffer) for 30 min at room temperature in a shaking water bath. Then, 150 μL of membrane/assay buffer mixture was added to wells containing 50 μL of drugs and [^{35}S]GTPγS [final concentrations: 20 mM Tris·HCl (pH 7.4), 100 mM NaCl, 5 mM $MgCl_2$, 0.1 mM DTT, 30–100 μM GDP, 0.1 nM [^{35}S]GTPγS, 0–30 μM [D-Ala^2, N-MePhe^4, Gly-ol]-enkephalin (DAMGO) or morphine, 10 μM modulator or DMSO to achieve 2% DMSO final concentration and either 15 μg of membrane protein per well for C6μ cell membranes or 10 μg of membrane protein per well for mouse brain membranes]. After incubation for an additional 5 min at room temperature, samples were quickly filtered through glass-fiber filter mats using a Brandel cell harvester and rinsed five times with ice-cold wash buffer [50 mM Tris·HCl (pH 7.4), 100 mM NaCl, 5 mM $MgCl_2$]. Filter mats were dried, scintillation mixture was added, and radioactivity retained on the filters was counted in a Wallac MicroBeta (PerkinElmer).

Data Analysis. Data from Fig. 2 were analyzed simultaneously with an allosteric ternary complex model in GraphPad Prism 5.01 (Dose–response–Special–Allosteric EC_{50} shift):

$$\begin{aligned}
&\text{Model :}\\
&EC_{50} = 10\text{^Log}EC_{50}\\
&K_b = 10\text{^Log}K_b\\
&\text{alpha} = 10\text{^Logalpha}\\
&\text{Antag} = (1 + B/K_b)/(1 + \text{alpha} \times B/K_b)\\
&\text{LogEC} = \text{Log}(EC_{50} \times \text{Antag})\\
&Y = \text{Bottom} + (\text{Top} - \text{Bottom})/(1 + 10\text{^}((\text{LogEC} - X)\\
&\qquad \times \text{HillSlope})),
\end{aligned}$$

where EC_{50} is the concentration of orthosteric agonist that produces a half maximal response in the absence of modulator. K_b is the equilibrium dissociation constant (molar) of modulator binding to its allosteric site. Alpha is the cooperativity factor. B is the concentration of allosteric modulator present. Top and Bottom are plateaus in the units of the Y axis.

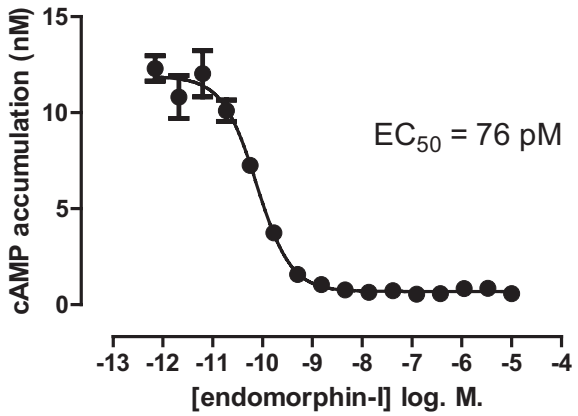

Fig. S1. Effect of endomorphin-I on inhibition of 1 μM forskolin-stimulated cAMP accumulation in CHO-μ cells. Endomorphin-I induced a 17-fold reduction in forskolin-stimulated cAMP accumulation with an EC_{50} of 76 pM [95% confidence interval (CI): 60–96 pM]. Data are represented as the means ± SEM of three experiments.

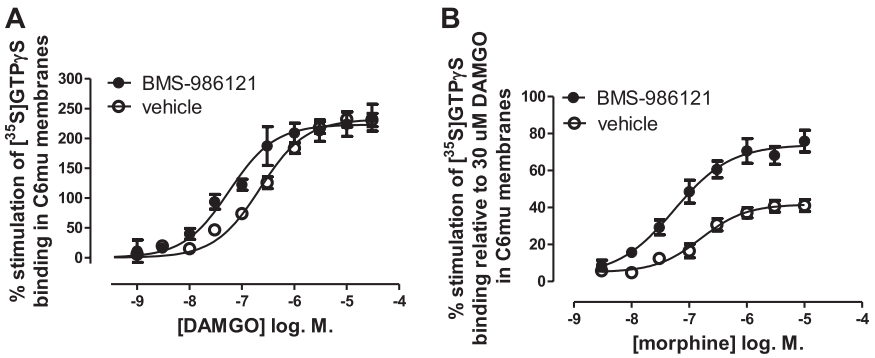

Fig. S2. Effect of μ-PAM, BMS-986121, on DAMGO-stimulated (*A*) and morphine-stimulated (*B*) [^{35}S]GTPγS binding in C6μ cell membranes. BMS-986121 (10 μM) resulted in a fourfold leftward shift in DAMGO potency. No significant agonist activity was detected for BMS-986121 (*A*). BMS-986121 (10 μM) increased morphine potency by 2.5-fold and increased the maximal effect (E_{max}) of morphine (*B*). Data are represented as the means ± SEM of three experiments.

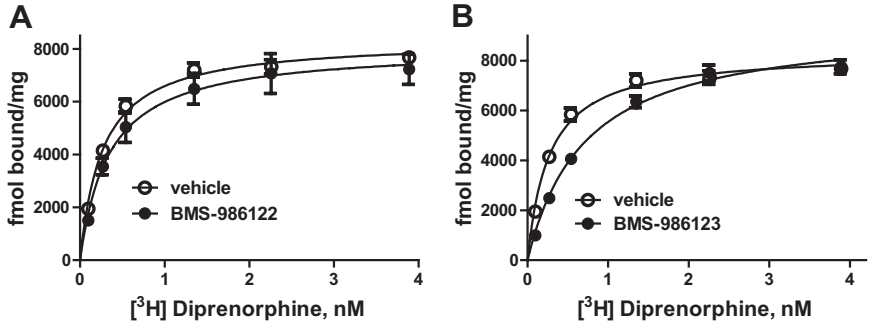

Fig. S3. Effect of the μ-PAM, BMS-986122, and the silent allosteric modulator (SAM), BMS-986123, on [^{3}H]diprenorphine saturation binding in membranes from C6μ cells. BMS-986122 (10 μM) (*A*) had no significant effect on [^{3}H]diprenorphine-binding affinity but induced a sixfold increase in the affinity of DAMGO in competition-binding studies (Fig. 4 and Table S1). BMS-986123 (10 μM) (*B*) produced a small (~twofold) but significant decrease in [^{3}H]diprenorphine affinity but had no significant effect on DAMGO affinity (Table S1). Data are represented as the means ± SEM of three to seven experiments.

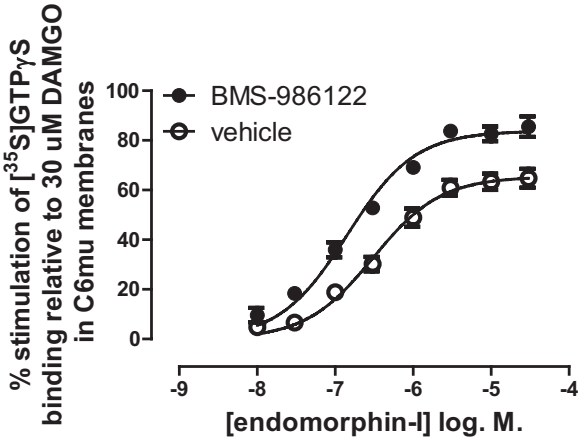

Fig. S4. Effect of μ-PAM, BMS-986122 (10 μM), on endomorphin-I–stimulated [^{35}S]GTPγS binding in C6μ membranes. Endomorphin-I was a partial agonist in this system relative to DAMGO. BMS-986122 (10 μM) increased the E_{max} of endomorphin-I compared with DAMGO [from 65% (95% CI: 62–69%) to 84% (95% CI: 80–87%)] and decreased the EC_{50} for endomorphin-I by twofold [from 307 nM (95% CI: 231–407 nM) to 143 nM (95% CI: 114–180 nM)]. Data are represented as the means ± SEM of three experiments.

	delta agonist mode	delta PAM mode	mu agonist mode	mu PAM mode	mu SAM mode
	% activity	% activity	% activity	% activity	% inhibition
Substance	U2OS-OPRD1	U2OS-OPRD1	U2OS-OPRM1	U2OS-OPRM1	U2OS-OPRM1
BMS-986122	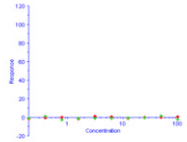	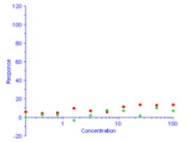	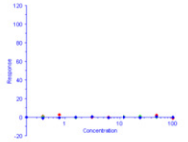	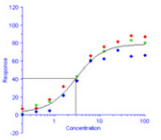	
Analog 1	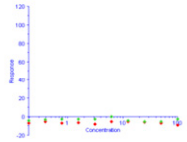	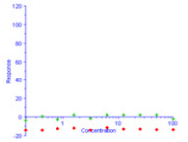	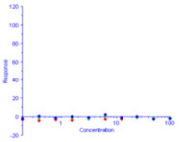	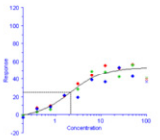	
Analog 2	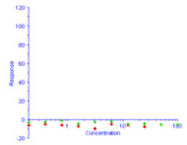	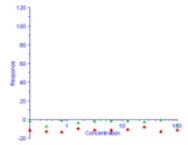	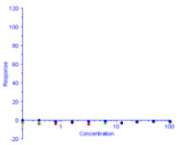	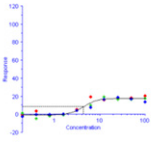	
Analog 3	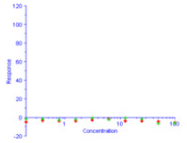	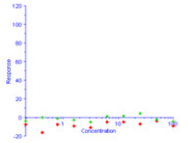	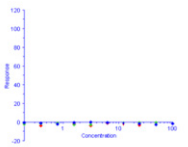	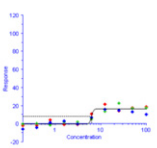	
Analog 4	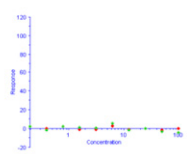	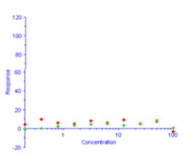	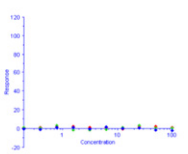	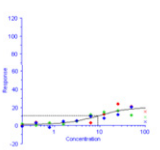	

Fig. S5. (Continued)

	delta agonist mode	delta PAM mode	mu agonist mode	mu PAM mode	mu SAM mode
	% activity	% activity	% activity	% activity	% inhibition
Substance	U2OS-OPRD1	U2OS-OPRD1	U2OS-OPRM1	U2OS-OPRM1	U2OS-OPRM1
Analog 5	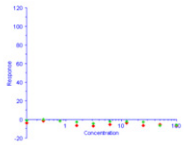	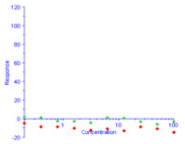	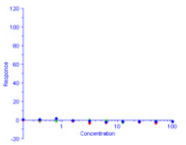	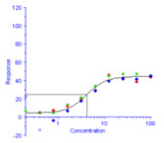	
Analog 6	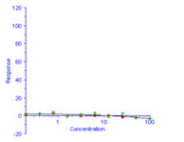	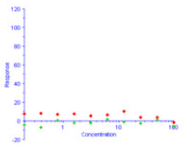	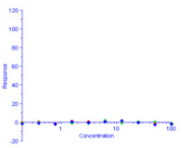	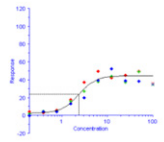	
Analog 7 (BMS-986123)	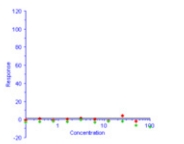	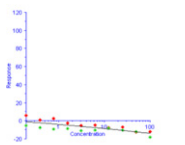	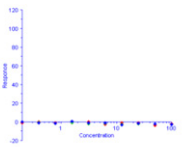	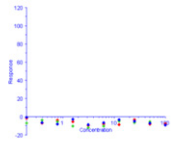	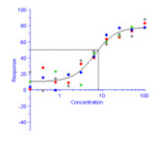
Analog 8	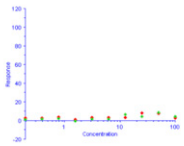	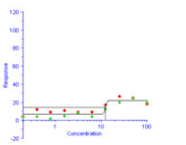	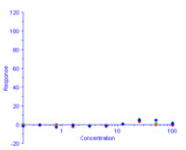	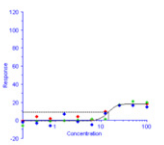	
Analog 9	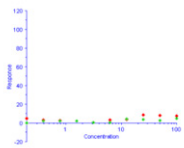	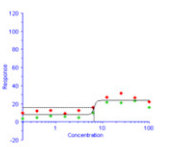	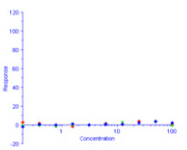	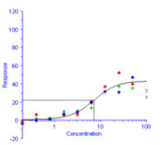	

Fig. S5. (Continued)

	delta agonist mode	delta PAM mode	mu agonist mode	mu PAM mode	mu SAM mode
	% activity	% activity	% activity	% activity	% inhibition
Substance	U2OS-OPRD1	U2OS-OPRD1	U2OS-OPRM1	U2OS-OPRM1	U2OS-OPRM1
Analog 10	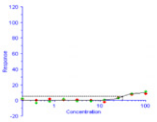	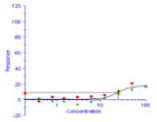	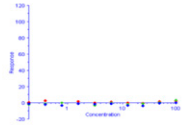	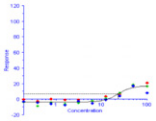	
Analog 11	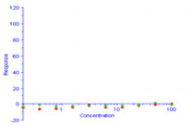	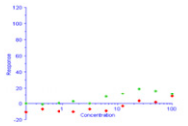	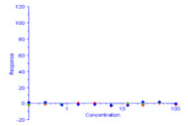	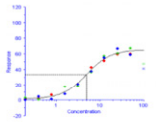	
Analog 12	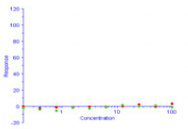	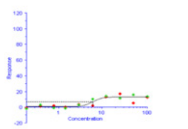	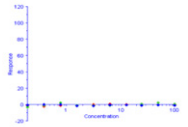	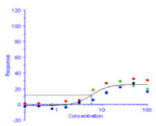	
Analog 13 (BMS-986124)	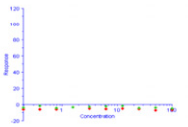	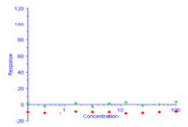	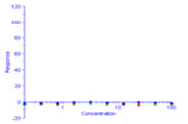	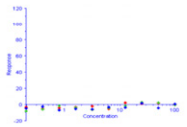	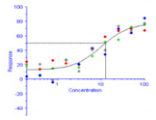
Analog 14	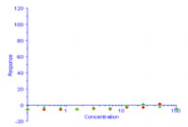	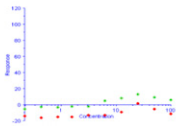	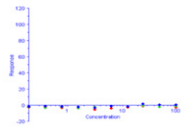	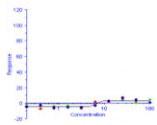	
Analog 15	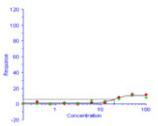	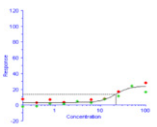	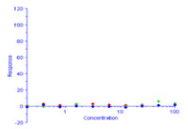	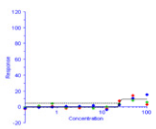	

Fig. S5. Activity of BMS-986122 and 15 analogs in a β-arrestin–recruitment assay in U2OS-OPRD1 and U2OS-OPRM1 cells. Compounds were tested in U2OS-OPRD1 cells in agonist-detection mode (in the absence of leu-enkephalin) and PAM-detection mode (in the presence of an ~EC_{10} concentration of leu-enkephalin). Compounds were also tested in U2OS-OPRM1 cells in agonist-detection mode (in the absence of endomorphin-I) and PAM-detection mode (in the presence of an ~EC_{10} concentration of endomorphin-I). Finally, compounds that exhibited no agonist or PAM activity in U2OS-OPRM1 cells were tested in SAM-detection mode (in the presence of an ~EC_{20} concentration of endomorphin-I plus an ~EC_{80} of the PAM BMS-986122). Graphical curve fit data are representative of three combined experiments. EC_{50} and E_{max} values are represented in Table S2. For agonist-detection mode, 0% and 100% activity represent basal activity and an E_{max} concentration of orthosteric agonist, respectively. For PAM-detection mode, 0% activity represents the response to a low (~EC_{10}) concentration of agonist alone, and 100% activity represents the response to an E_{max} concentration of agonist. For SAM-detection mode, 0% inhibition represents the response to a low (~EC_{20}) concentration of endomorphin-I combined with an ~EC_{80} concentration of the μ-PAM BMS-986122; 100% inhibition represents the response to a low (~EC_{20}) concentration of endomorphin-I alone.

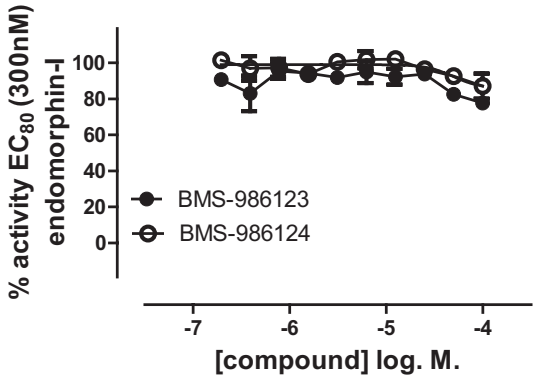

Fig. S6. Effect of BMS-986123 and BMS-986124 on β-arrestin response to an ~EC_{80} concentration of endomorphin-I (antagonist/NAM-detection mode) in U2OS-OPRM1 cells. BMS-986123 and BMS-986124 had no significant effect on endomorphin-I –mediated (300 nM) β-arrestin activity in U2OS-OPRM1 cells; 100% activity is normalized to the response to endomorphin-I (300 nM) alone; 0% activity represents basal activity. Data are represented as the means ± SEM of three experiments.

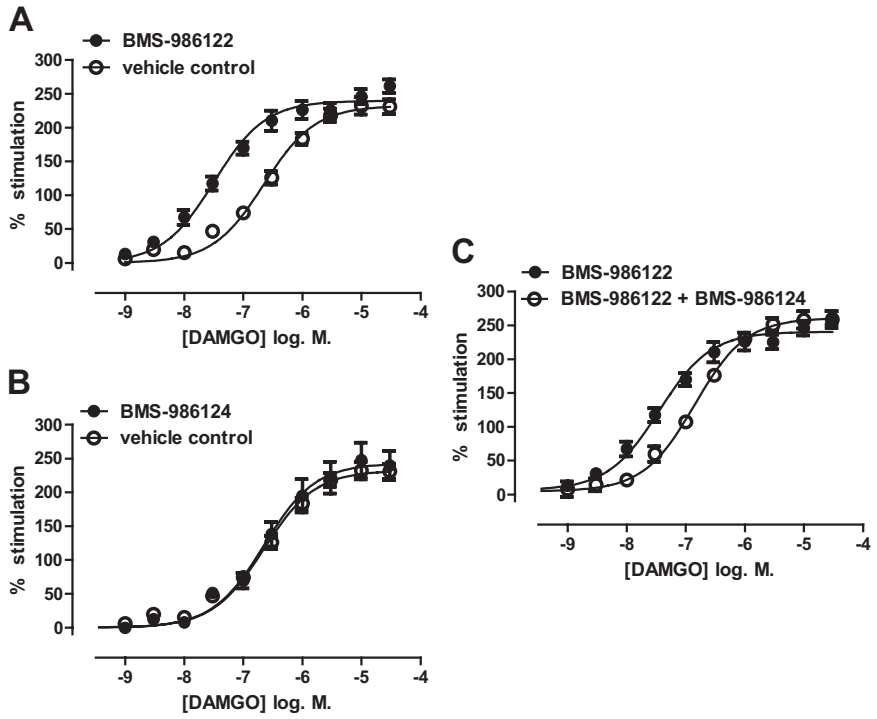

Fig. S7. Effect of BMS-986124 on BMS-986122–mediated PAM activity to DAMGO-stimulated [^{35}S]GTPγS binding in C6μ cell membranes. DAMGO-stimulated [^{35}S]GTPγS-binding potency in C6μ membranes was increased eightfold in the presence of the μ-PAM BMS-986122 (10 μM) (*A*). DAMGO-stimulated [^{35}S]GTPγS-binding potency was not affected by incubation with 50 μM BMS-986124 (*B*). Coincubation of BMS-986124 (50 μM) with BMS-986122 (10 μM) resulted in a rightward shift in DAMGO potency compared with incubation with BMS-986122 alone (*C*). The potency of DAMGO in the presence of both BMS-986122 and BMS-986124 was shifted leftward by only twofold compared with DAMGO potency in the presence of the vehicle control. These data suggest that BMS-986124 can antagonize the BMS-986122 PAM effect. Shown are the combined means ± SEM data from three to seven separate assays, each performed in duplicate. EC_{50} values are given in *Results and Discussion* and in Fig. 5*B*.

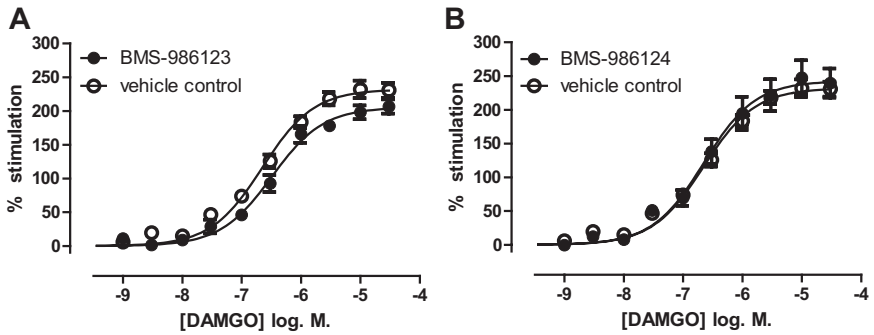

Fig. S8. Effect of the SAMs, BMS-986123 and BMS-986124, on DAMGO-stimulated [^{35}S]GTPγS binding above basal activity in membranes from C6μ cells. DAMGO potency [EC_{50} of 222 nM (95% CI: 179–274 nM)] was not significantly affected by BMS-986123 (*A*) [EC_{50} of 321 nM (95% CI: 239–432 nM] or BMS-986124 (*B*) [EC_{50} of 223 nM (95% CI: 150–331 nM)]. The maximal stimulation by DAMGO [control max, 232% (95% CI: 223–242%)] was not affected by BMS-986124 [243% (95% CI: 224–262%)]. Maximal stimulation was decreased slightly by BMS-986123 [206% (95% CI: 193–218%)]. The modulators did not significantly affect the basal values (vehicle control basal, 3.2 ± 0.2 fmol bound per milligram of protein). Shown are the combined data from three to seven separate assays, each performed in duplicate.

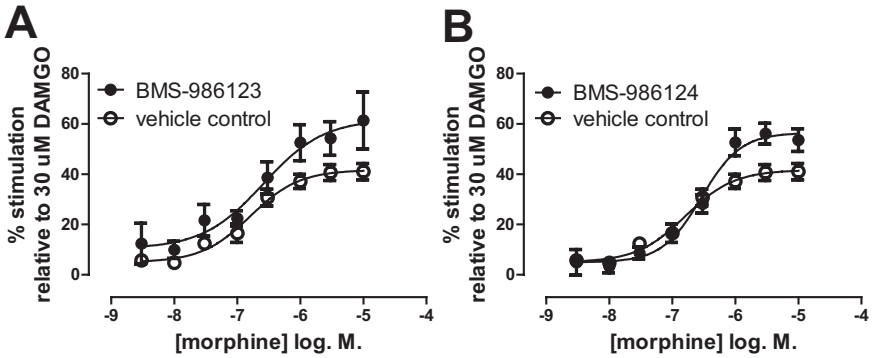

Fig. S9. Effect of the SAMs BMS-986123 and BMS-986124 on morphine-stimulated [^{35}S]GTPγS binding in membranes from C6μ cells. The EC_{50} of morphine to stimulate [^{35}S]GTPγS binding [110 nM (95% CI: 71–171 nM)] was not significantly affected by BMS-986123 (*A*) [140 nM (95% CI: 67–293 nM)] but was decreased by BMS-986124 (*B*) [245 nM (95% CI: 161–372 nM)]. The E_{max} of morphine compared with DAMGO (30 μM) [control max, 42% (95% CI: 38–45%)] was increased to a small degree by BMS-986123 [62% (95% CI: 52–73%)] and BMS-986124 [58% (95% CI: 53–64%)]. Shown are the combined data from three to seven separate assays, each performed in duplicate.

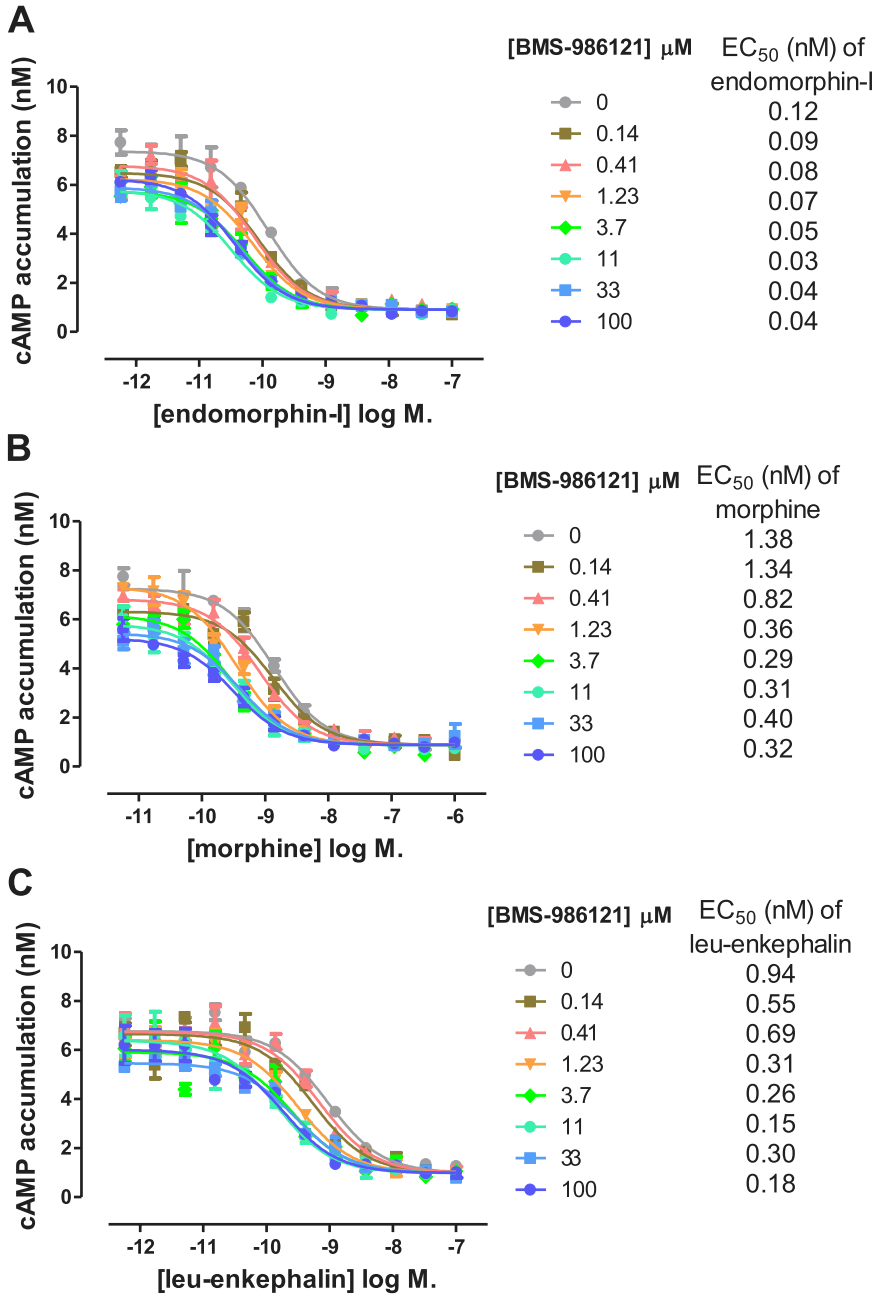

Fig. S10. Effect of μ-PAM BMS-986121 on inhibition of forskolin-stimulated cAMP accumulation, mediated by different orthosteric agonists, in CHO-μ cells. BMS-986121 (100 μM) produced leftward shifts in agonist potency for each of the three orthosteric ligands used [endomorphin-I, fourfold (*A*); morphine, fivefold (*B*); and leu-enkephalin, fivefold (*C*)]. EC_{50} values for the agonists at each BMS-986121 concentration are shown in the legend. Data represent the means ± SEM of three experiments.

Table S1. Effect of the μ-PAM BMS-986122 and the SAM BMS-986123 on [^{3}H]diprenorphine saturation binding and DAMGO competition binding in membranes from C6μ cells

Compound added	[^{3}H]diprenorphine, K_d nM, mean (95% CI)	DAMGO, K_i nM, mean (95% CI)
Vehicle control in Tris·HCl + sodium and GTP analogs	0.27 (0.21–0.32)	340 (208-552)
BMS-986122 (10 μM) in Tris·HCl + sodium and GTP analogs	0.35 (0.18–0.51)	56 (41-76)
BMS-986122 (100 μM) in Tris·HCl + sodium and GTP analogs	0.34 (0.13–0.55)	ND
BMS-986123 (10 μM) in Tris·HCl + sodium and GTP analogs	0.71 (0.57–0.86)	270 (179-406)
Vehicle control in Tris·HCl buffer	0.22 (0.02–0.46)	2.21 (1.51–3.23)
BMS-986122 (10 μM) in Tris·HCl buffer	0.23 (0.04–0.43)	0.51 (0.36–0.72)

ND, not determined.

Table S2. Structure–activity relationship of BMS-986122 and analogs tested in the β-arrestin–recruitment assay in U2OS-OPRM1 cells, in PAM-detection mode

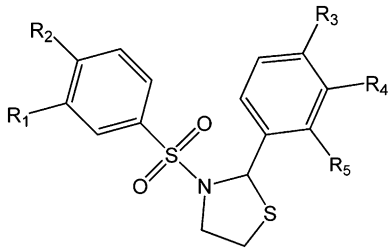

Substance	R1	R2	R3	R4	R5	β-Arrestin PAM-detection mode, % E_{max}	β-Arrestin PAM-detection mode, EC_{50} (μM)	Description	β-Arrestin SAM detection mode, K_b (μM)
BMS-986122	H	Cl	OMe	Br	H	79	3	Full PAM (ref)	
Analog 1	H	Nitro	OMe	Br	H	53	2	Moderate PAM	
Analog 2	H	Me	OMe	Br	H	18	4	Weak PAM	
Analog 3	H	OMe	OMe	Br	H	16	6	Weak PAM	
Analog 4	Me	H	OMe	Br	H	20	9	Weak PAM	
Analog 5	H	Cl	OMe	Nitro	H	45	4	Moderate PAM	
Analog 6	H	Br	OMe	Nitro	H	45	2	Moderate PAM	
Analog 7 (BMS-986123)	H	Me	OMe	Nitro	H	—	—	SAM	1
Analog 8	H	Br	OMe	OMe	H	18	14	Weak PAM	
Analog 9	H	Br	OMe	H	H	44	7	Moderate PAM	
Analog 10	H	H	OMe	H	H	17	23	Weak PAM	
Analog 11	H	Cl	H	Cl	H	65	5	Strong PAM	
Analog 12	H	Cl	Br	H	H	26	6	Weak PAM	
Analog 13 (BMS-986124)	H	Cl	Br	H	OMe	—	—	SAM	2
Analog 14	H	OMe	Br	H	H	3	7	Weak PAM	
Analog 15	H	OMe	OMe	H	H	9	37	Weak PAM	

Compounds exhibiting PAM activity were described based on their efficacy as full, strong, moderate, or weak PAMs; 0% activity represents the response to a low (~EC_{10}) concentration of endomorphin-I alone, and 100% activity represents the response to an E_{max} concentration of endomorphin-I. The two compounds that showed no PAM activity were additionally tested in SAM-detection mode [inhibition of BMS-986122 (~EC_{80}) response in the presence of a low concentration (~EC_{20}) of endomorphin-I], where the compounds were shown to inhibit the BMS-986122 response (Fig. S5). Calculated K_b values are provided from IC_{50} values. Concentration response curves for the SAM compounds, BMS-986123 and BMS-986124, are shown in Fig. 5*A*. Data are represented as the means of three experiments.—, not active.